AGU PUBLICATIONS

Global Biogeochemical Cycles

RESEARCH ARTICLE
10.1002/2015GB005280

Key Points:
- The terrestrial environment is the largest net source of total Hg to the Arctic Ocean
- Atmospheric MeHg from oceanic Me_2Hg evasion may be the largest source to the surface ocean
- Geochemical modeling shows Hg in the upper ocean responds rapidly to changing inputs

Supporting Information:
- Tables S1–S9, Texts S1 and S2, and Figures S1–S4

Correspondence to:
A. L. Soerensen,
anne.soerensen@aces.su.se

Citation:
Soerensen, A. L., D. J. Jacob, A. T. Schartup, J. A. Fisher, I. Lehnherr, V. L. St. Louis, L.-E. Heimbürger, J. E. Sonke, D. P. Krabbenhoft, and E. M. Sunderland (2016), A mass budget for mercury and methylmercury in the Arctic Ocean, *Global Biogeochem. Cycles*, *30*, doi:10.1002/2015GB005280.

Received 8 SEP 2015
Accepted 1 FEB 2016
Accepted article online 3 FEB 2016

A mass budget for mercury and methylmercury in the Arctic Ocean

Anne L. Soerensen[1,2,3], Daniel J. Jacob[2], Amina T. Schartup[1,2], Jenny A. Fisher[4], Igor Lehnherr[5,6], Vincent L. St. Louis[5], Lars-Eric Heimbürger[7,8,9], Jeroen E. Sonke[7], David P. Krabbenhoft[10], and Elsie M. Sunderland[1,2]

[1]Harvard T.H. Chan School of Public Health, Department of Environmental Health, Boston, Massachusetts, USA, [2]Harvard University, John A. Paulson School of Engineering and Applied Sciences, Cambridge, Massachusetts, USA, [3]Stockholm UniversityDepartment of Environmental Science and Analytical Chemistry, Stockholm, Sweden, [4]University of Wollongong, Centre for Atmospheric Chemistry, Wollongong, New South Wales, Australia, [5]University of Alberta, Department of Biological Sciences, Edmonton, Alberta, Canada, [6]University of Toronto-Mississauga, Department of Geography, Mississauga, Ontario, Canada, [7]CNRS, Geoscience Environment Toulouse, Midi-Pyrenees Observatory, Toulouse, France, [8]University of Bremen, Department of Geosciences, Bremen, Germany, [9]Aix Marseille Université, CNRS/INSU, Université de Toulon, IRD, Mediterranean Institute of Oceanography UM 110, Marseille, France, [10]U.S. Geological Survey, Middleton, Wisconsin, United States

Abstract Elevated biological concentrations of methylmercury (MeHg), a bioaccumulative neurotoxin, are observed throughout the Arctic Ocean, but major sources and degradation pathways in seawater are not well understood. We develop a mass budget for mercury species in the Arctic Ocean based on available data since 2004 and discuss implications and uncertainties. Our calculations show that high total mercury (Hg) in Arctic seawater relative to other basins reflect large freshwater inputs and sea ice cover that inhibits losses through evasion. We find that most net MeHg production (20 Mg a^{-1}) occurs in the subsurface ocean (20–200 m). There it is converted to dimethylmercury (Me_2Hg: 17 Mg a^{-1}), which diffuses to the polar mixed layer and evades to the atmosphere (14 Mg a^{-1}). Me_2Hg has a short atmospheric lifetime and rapidly degrades back to MeHg. We postulate that most evaded Me_2Hg is redeposited as MeHg and that atmospheric deposition is the largest net MeHg source (8 Mg a^{-1}) to the biologically productive surface ocean. MeHg concentrations in Arctic Ocean seawater are elevated compared to lower latitudes. Riverine MeHg inputs account for approximately 15% of inputs to the surface ocean (2.5 Mg a^{-1}) but greater importance in the future is likely given increasing freshwater discharges and permafrost melt. This may offset potential declines driven by increasing evasion from ice-free surface waters. Geochemical model simulations illustrate that for the most biologically relevant regions of the ocean, regulatory actions that decrease Hg inputs have the capacity to rapidly affect aquatic Hg concentrations.

1. Introduction

Accumulation of methylmercury (MeHg) in Arctic biota is a major concern for the health of northern populations that consume large quantities of marine foods [*Arctic Monitoring and Assessment Programme (AMAP)*, 2011a; *Riget et al.*, 2011b]. High MeHg concentrations in Arctic fish and marine mammals have been attributed to a combination of enhanced mercury (Hg) deposition at high latitudes and enhanced biomagnification due to climate-driven shifts in ocean biogeochemistry and trophic structure [*Braune et al.*, 2015; *Stern et al.*, 2012]. Prior work has characterized total mercury (Hg) inputs and reservoirs in the Arctic Ocean but has not quantified the link to bioaccumulative MeHg [*Fisher et al.*, 2013; *Kirk et al.*, 2012; *Outridge et al.*, 2008; *Zhang et al.*, 2015]. Here we use available measurement data since 2004 to construct Arctic Ocean mass budgets for Hg and MeHg and gain insight into processes driving MeHg concentrations in Arctic Ocean seawater.

In marine ecosystems, MeHg is produced from divalent inorganic Hg (Hg^{II}) by bacteria in benthic sediment and in the water column [*Lehnherr*, 2014]. It is also produced in freshwater ecosystems and wetlands and transported by rivers into the surface ocean [*Nagorski et al.*, 2014]. *Lehnherr et al.* [2011] measured water column methylation at the subsurface chlorophyll maximum and the oxycline at multiple stations in the Canadian Arctic Archipelago and concluded that this is likely the major MeHg source to polar marine waters. Levels of dimethylmercury (Me_2Hg) measured in Arctic surface seawater (Table 1) are high compared to other oceans [*Bowman et al.*, 2015; *Horvat et al.*, 2003]. Incubation experiments show Me_2Hg is mainly produced from MeHg in seawater [*Lehnherr et al.*, 2011]. Recent measurements have identified evaded Me_2Hg from the

Table 1. Measured Concentrations of Hg Species in Arctic Ocean Seawater[a]

Region	Total Hg (pM)	Methylated Hg (fM)	Fraction Methylated (%)	Me_2Hg (fM)	Hg^0 (fM)
Polar mixed layer (<20 m)	1.56 ± 0.32[b]	64 ± 43[b]	4.5 ± 3.4[b]	60 ± 70[d]	126 ± 51[d]
	2.92 ± 2.88[d]	141 ± 79[d]	5[d]	55 ± 20[k]	220 ± 110[e]
	2.09 ± 1.85[c]	474 ± 70[k]	45.2[k]	37[g]	643 ± 179[k]
	0.55–1.40[f]	284, 454, and 364[l]	30–40[l]	50[h]	30[g]
	0.70–1.20[k]	102[g]	5.5[g]	168[i]	89[h]
	2.29 ± 2.00[g]	105 ± 61[h]	4.4[h]	34 ± 30[m]	127[i]
	1.91 ± 9.24[h]	250[i]	13.7[i]	17 ± 10[n]	
	1.82 ± 0.45[i]	122[m]			
		146[n]			
Best Estimate	**2.0 ± 1.8**	**130 ± 110**	**7%**	**50 ± 40**	**180 ± 90**
		90 ± 70 (MeHg)			
Subsurface Ocean	1.10 ± 0.20[b]	216 ± 95[b]	19.3 ± 7.3[b]	362 ± 184[d]	171 ± 149[d]
(20 shelf bottom or 200 m)	1.43 ± 1.11[d]	445 ± 180[d]	31[d]	277[g]	82[g]
	2.02 ± 0.52[g]	407[g]	20[g],	331[h]	48[h]
	1.92 ± 0.32[h]	627[h]	33[h]	427[i]	103[i]
	1.57 ± 0.31[i]	517[i]	33[i]	138[m]	
	1.1 ± 0.45[j]	200 ± 150[j]	18 ± 14[j]	65[n]	
		248[m]			
		212[n]			
Best Estimate	**1.3 ± 0.5**	**320 ± 220**	**25%**	**220 ± 150**	**110 ± 70**
		110 ± 70 (MeHg)			
Deep Central Basin	1.0 ± 0.3[b]	201 ± 86[b]	20.6 ± 9.5[b]		
and Baffin Bay (>200 m)					
Best Estimate	**1.0 ± 0.3**	**200 ± 90**	**20%**		

[a]NA = not available. Best estimate is used in mass budget calculations and calculated based on raw data from individual profiles from the cruises presented here. The Hg^0 reservoir in the PML is estimated by subtracting Me_2Hg concentrations from measured dissolved gaseous mercury (DGM). DGM and Me_2Hg observations are from a mix of ice-free and ice-covered stations. The best estimate of MeHg concentrations in the upper ocean is based on the ratio of MeHg:Me_2Hg (PML: 2:1 and subsurface: 0.7:1) [Lehnherr et al., 2011]. Cruise tracks for observations are shown in Figure 1

[b]August–September 2011 Cruise in the Central Basin [*Heimbürger et al.*, 2015].

[c]Baffin Bay July 2008 [*Zdanowicz et al.*, 2013].

[d]Canadian Arctic Archipelago/border to Baffin Bay August–October 2005 (stations 1–11) [*Kirk et al.*, 2008].

[e]July–September measurements in Baffin Bay, Shelf, and Central Arctic Basin reported as DGM (Hg^0 + Me_2Hg) [*Andersson et al.*, 2008].

[f]Canadian Arctic Archipelago, March–May 2008 [*Chaulk et al.*, 2011].

[g]Canadian Arctic Archipelago, October 2007 [*Lehnherr et al.*, 2011].

[h]Canadian Arctic Archipelago, September 2006 (supporting information Text S2).

[i]Canadian Arctic Archipelago, August 2010 (supporting information Text S2).

[j]Beaufort Sea, March–July 2008 [*Wang et al.*, 2012].

[k]Canadian Arctic Archipelago May 2004 [*St Louis et al.*, 2007].

[l]Canadian Arctic Archipelago May 2005 [*St Louis et al.*, 2007].

[m]Canadian Arctic Archipelago July–August 2010 [*Baya et al.*, 2015].

[n]Canadian Arctic Archipelago July–August 2011 [*Baya et al.*, 2015].

Arctic surface ocean and subsequent atmospheric MeHg deposition as a substantial source to ocean surface waters and adjacent terrestrial ecosystems [*Baya et al.*, 2015; *Lin and Pehkonen*, 1999; *St Pierre et al.*, 2015].

Concentrations of total Hg are elevated in Arctic surface seawater relative to other basins [*Heimbürger et al.*, 2015; *Mason et al.*, 2012]. Sea ice cover, an extensive continental shelf, large freshwater inputs, and salinity-driven stratification of the surface mixed layer distinguish the Arctic Ocean from the midlatitude oceans. Springtime releases of bromine result in rapid oxidation of gaseous elemental Hg (Hg^0) to the water-soluble divalent species (Hg^{II}) and atmospheric Hg depletion events (AMDEs) [*Schroeder et al.*, 1998; *Steffen et al.*, 2015]. AMDEs were originally hypothesized to drive large increases in oceanic Hg inputs, but subsequent work shows that approximately half of the deposited Hg^{II} is reemitted back to the atmosphere after photochemical reduction in the surface ocean and snowpack [*Dastoor et al.*, 2015; *Kirk et al.*, 2006; *Lalonde et al.*, 2002]. Rivers are a large source of total Hg to the Arctic Ocean, but prior modeling work has not evaluated their importance for MeHg cycling [*Dastoor and Durnford*, 2014; *Fisher et al.*, 2012; *Outridge et al.*, 2008; *Zhang et al.*, 2015].

Here we develop a five-box geochemical model for the Arctic Ocean parameterized using Hg and MeHg measurements collected over the last decade (2004–2014). We force the model with changes in sea ice since 1975 and modeled anthropogenic Hg deposition between 1850 and 2010. We use this analysis to gain insight into processes affecting MeHg concentrations in Arctic Ocean biota and timescales of response associated with

Table 2. Measured Concentrations of Hg Species in Ice, Suspended Particles in the Water Column, Benthic Sediment and Air from the Arctic Ocean[a]

Medium	Total Hg	MeHg	Fraction MeHg (%)
Ice (pM)	4.0, 5.6, and 12.7 (0.65–61)[b] 0.5–4.0, max 20[c] 3.9 ± 1.0[d]	0.2 and 1.35 (<0.10–2.64)[b]	3.5–10[b]
Best estimate	**7.4 (2.8–10.0)**	**0.75 (0.15–1.3)**	**10%**
Suspended solids (ng g^{-1} dry weight)	33 ± 26 (4–88)[e] 36 ± 27[g] 74 ± 27 (45–98)[h]	1.4 ± 1.1 (0.15–3.51)[e] 1.1[f] <0.15[g] 3.7 ± 1.0 (2.6–4.4)[h]	<4[e] <0.5[f]
Best estimate	**50 (30–70)**	**2 (0.15–3.51)**	**4%**
Shelf sediment (ng g^{-1} dry weight)	31 ± 10 (5–55)[i] 50–100[j] 23 (8–40)[l] 41 ± 29[m] 54 ± 23[n]	0.15 ± 0.07 (0.03–0.29)[i] 0.05–0.37[j] 0.37 ± 0.36 (<0.01-1.41)[k]	0.43 ± 0.17[i] ~0.05–0.20[j] 0.70 ± 0.40[k]
Best estimate	**45 (23–65)**	**0.2 (0.1–0.3)**	**0.4%**
Central Basin/Baffin Bay sediment (ng g^{-1} dry weight)	<50–70[o]	<0.05–0.10[o]	~0.05[o]
Best estimate	**45 (23–65)**	**0.05 (0.01–0.10)**	**0.1%**
Marine boundary layer	1.7 ± 0.4 (ng Hg^0 m^{-3})[p]	3.8 ± 3.1 (pg Me_2Hg m^{-3})[q]	
Best Estimate	**1.7**	**3.8**	

[a]Best estimate for mass budget calculations are based on campaign averages and midpoints of reported ranges where raw data are not available.
[b]Multitear sea ice from three cores in the Beaufort Sea in May, August, and September [*Beattie et al.*, 2014].
[c]Multiyear sea ice from the Canadian Arctic Archipelago in May [*Chaulk et al.*, 2011].
[d]Multiyear sea ice from the Canadian Arctic Archipelago in June [*Poulain et al.*, 2007].
[e]Total suspended solids from the Canadian Arctic Archipelago [*Burt*, 2012].
[f]Total suspended solids from the Canadian Arctic Archipelago (supporting information Text S2).
[g]Particulate organic matter from the Canadian Arctic Archipelago [*Pucko et al.*, 2014].
[h]Total suspended solids in the Beaufort Sea [*Graydon et al.*, 2009].
[i]Benthic sediment Chukchi Sea [*Fox et al.*, 2013].
[j]Benthic sediment Chukchi Sea and Yermak Plateau [*Kading and Andersson*, 2011].
[k]Benthic sediment Beaufort Sea [*Fox et al.*, 2013].
[l]Bering Sea upper 1–2 cm benthic sediment from 2004, 2006, and 2009 (ICES Data Portal, Contaminants and biological effects of contaminants on sediments, ICES, Copenhagen, http://ecosystemdata.ices.dk/ Extraction).
[m]Upper 2 cm Beaufort Sea benthic sediment [*Trefry et al.*, 2003].
[n]Canadian Arctic Archipelago >65 N benthic surface sediment [*Canario et al.*, 2013].
[o]Central Basin surface sediment [*Kading and Andersson*, 2011].
[p]*Sommar et al.* [2010].
[q]*Baya et al.* [2015].

changes in external Hg sources. We develop hypotheses about key biogeochemical processes that can be tested in future research and discuss major uncertainties and data gaps.

2. Model Overview

Our five-box geochemical model for the Arctic Ocean includes compartments representing (1) the upper 20 m of the water column known as the polar mixed layer (PML) defined based on an observed density gradient of 0.01 kg m^{-3} [*Toole et al.*, 2010] and consistent with previous model representations [*Fisher et al.*, 2012; *Fisher et al.*, 2013]; (2) the subsurface ocean that extends to the bottom on the shelf and to 200 m depth in the Central Arctic Basin and Baffin Bay [*Pickard and Emery*, 1990]; (3) the deep ocean below 200 m to the sea floor in the central Basin and Baffin Bay; (4) active sediment layers on the shelf (2 cm) and in the Central Basin (1 cm). The active sediment layer depth characterizes benthic sediment that interacts with the water column through bioturbation/resuspension and chemical diffusion [*Clough et al.*, 1997; *Kuzyk et al.*, 2013; *Trefry et al.*, 2014].

We estimate external inputs and exchanges/loss of Hg species (Hg^{II}, Hg^0, MeHg, and Me_2Hg) from each compartment based on a comprehensive review of measured concentrations and fluxes (Tables 1–4). We assessed

Table 3. Physical Characteristics of Arctic Ocean Basin Used to Develop Mass Budgets for Hg Species

Parameter	Value	Reference
Volume of Arctic Ocean (m^3)	136×10^{14}	*Jakobsson* [2002]
Volume of polar mixed layer (0–20 m) (m^3)	2.22×10^{14}	*Jakobsson* [2002]
Volume of middepth water (shelf: 20 bottom; Central Basin and Baffin Bay: 20–200 m) (m^3)	16.1×10^{14}	*Jakobsson* [2002]
Volume of water below 200 meters (m^3)	118×10^{14}	*Jakobsson* [2002]
Volume of sea ice (m^3)	0.1×10^{14}	*Serreze et al.* [2006]
Volume of active shelf sediment (m^3) (0.02 m depth)	18×10^{10}	
Volume of active deep sediment (m^3) (0.01 m depth)	5×10^{10}	
Surface area of shelf regions (m^2)	608×10^{10}	*Jakobsson* [2002]
Surface area of the Central Basin and Baffin Bay (m^2)	500×10^{10}	*Jakobsson* [2002]
Total Arctic surface area (m^2)	1109×10^{10}	*Jakobsson* [2002]
Bacterial biomass (g C m^{-2})	0.34	*Kirchman et al.* [2009]
Phytoplankton shelf biomass (g C m^{-2})	1.75 (1.00–2.50)	*Kirchman et al.* [2009]
Phytoplankton Central Basin biomass (g C m^{-2})	0.50	*Kirchman et al.* [2009]
Zooplankton shelf biomass (<82°N) (g dw m^{-2})	6.9 ± 4.1	*Kosobokova and Hirche* [2009]
Zooplankton Central Basin biomass (>82°N) (g dw m^{-2})	2.5 ± 0.5	*Kosobokova and Hirche* [2009]
Zooplankton [MeHg], best estimate (ng g dw^{-1})	11 (5–35)	Table S2
Carbon to dry weight plankton	2	*Hedges et al.* [2002] and *Redfield et al.* [1963]
Average precipitation (mm)	340	*Serreze et al.* [2006]
Fraction of summer precipitation	0.6	*Serreze and Barry* [2005]
Fraction of ice-free water in summer (Apr–Sept, average)	0.65	*Macdonald et al.* [2005] and *National Snow and Ice Data Center (NSIDC)* [2013]
Fraction of ice-free water in winter (Oct–March, average)	0.10	*Macdonald et al.* [2005] and *National Snow and Ice Data Center (NSIDC)* [2013]
Shelf sediment burial rate (m a^{-1})	30×10^{-5}	*Kuzyk et al.* [2013], *Pirtle-Levy et al.* [2009], *Polyak et al.* [2009]
MeHg (Hg^{II}) deposition velocity (cm s^{-1})	1	*Zhang et al.* [2009]
Deep sediment burial rate (m a^{-1})	3×10^{-5}	*Polyak et al.* [2009]
Average concentration of Chl *a* in mixed layer (mg/L)	0.6×10^{-3}	*Galand et al.* [2008] and *Jin et al.* [2012]
Average summer shortwave radiation (W m^{-2})	160	*Hatzianastassiou et al.* [2005]
Concentration of DOC in water column (mg L^{-1})	0.8	*Dittmar and Kattner* [2003] and *Hansell et al.* [2012]
Net primary production (g C m^{-2} d^{-1})	0.28	*Arrigo and van Dijken* [2011] and *Hill et al.* [2013]
Average wind speed at 10 m above sea surface (m s^{-1})	5.6 (4–6)	*Nummelin et al.* [2015] and *Serreze and Barry* [2005]

the quality (detection limits and QA/QC) of all data prior to incorporation in data tables. The choice to focus on data collected after 2004 was made to minimize sample contamination known to have prevalently occurred in earlier decades in addition to representing current conditions. Mass budgets for each species are used to derive first-order rate coefficients and create a set of coupled first-order differential equations to be able to simulate changes in chemical mass over time following *Sunderland et al.* [2010]. Processes in the model include (1) external inputs from atmospheric deposition, rivers, erosion, snow and ice melt, and other oceans, (2) advective transport by seawater circulation, ice transport, and settling of suspended particulate matter, (3) diffusive transport through the water column and at the sediment-water and air-sea interfaces, and (4) chemical transformations through inorganic Hg redox reactions and methylation, and degradation of MeHg and Me_2Hg. Details of mass budget calculations are provided in the Tables S3–S9 in the supporting information.

2.1. Hydrologic and Solids Budget

Hydrologic and solids budgets used to characterize advective transport of Hg species are provided in the supporting information (Figure S1). The hydrologic budget is based on seawater inflow and outflow from the

Table 4. External Inputs of Hg Species to the Arctic Ocean[a]

Medium	Total Hg	MeHg	Fraction MeHg (%)
Rain and fresh snow (pM)	2.6 ± 0.75[b]	0.13 ± 0.05[c] 0.80 ± 0.35[b] 0.50[d]	30[b]
XBest estimate for wet deposition (pM)		**0.50 (0.15-0.80)**	
Surface snow (p*M*)	15.8 ± 15.5[e] 35.7[f] 3.5 ± 2.8[g] 10.2 ± 3.5[h]	0.25 ± 0.95[e] 0.1[f] 0.35 ± 0.15[g]	1.6[e] 0.2[f] 10[g]
Snowpack (p*M*)	39[j] 2.6–8.8[k] 6.7–19.4[l] 10–250[m] 170[n]	0.37 ± 0.10[i] 0.35–0.43[k] <0.08–0.10[l]	21–31[k]
Runoff (p*M*)	3.6 ± 0.8[o] 5.8 ± 4.8[p] 10.1 ± 3.2[p]	0.77 ± 0.41[o] 0.31 ± 0.19[q]	19.9[o] 3.2[q]
Best Estimate for melt water (pM)	**15 (2.5–30)**	**0.3 (0.1–0.7)**	**5 (2–20)**
Rivers and rivulets (p*M*)	45.7 ± 27.5[r] 61.3 ± 8.2[s] 35.8[t] 33.5–67.7[u] 73[w] 31, 39, 24, 18, and 14[x]	~0.35[r] 0.35 ± 0.05[s] 0.10 ± 0.10[v]	1.1 (5.2 shelf)[r] 0.2–1.5[s] 1.3[v]
Best Estimate for rivers (pM)			**5 (1–10)**
Erosion (ng g^{-1})	114, 61, and 67[y]		0.5–2.0[z]
Best Estimate for erosion (ng g^{-1})	**81 (61–114)**		**1.0**

[a]Best estimate is computed as the mean of average values from reported campaigns. Supporting information Figures S2 and S3 report uncertainty ranges on reservoirs and fluxes not given here.
[b]Fresh snow from Baffin Bay collected in April [*Zdanowicz et al.*, 2013].
[c]Rain collected from the Canadian Arctic Archipelago collected in June [*Hammerschmidt et al.*, 2006].
[d]Rain collected from the Canadian Arctic Archipelago collected in July [*Lehnherr et al.*, 2012].
[e]Surface snow from the Canadian Arctic Archipelago collected in April and May [*St Louis et al.*, 2005].
[f]Surface snow from the Canadian Arctic Archipelago collected In May (median) [*St Louis et al.*, 2007].
[g]Surface snow from Baffin Bay collected in April [*Zdanowicz et al.*, 2013].
[h]Surface snow from the Canadian Arctic Archipelago collected in June [*Poulain et al.*, 2007].
[i]Fall-winter snowpack from the Canadian Arctic Archipelago [*St Louis et al.*, 2005].
[j]Fall-winter snowpack from the Central Basin collected in November–January [*Lu et al.*, 2001].
[k]Spring snowpack from the Canadian Arctic Archipelago in April-May (means), first & second year snow [*St Louis et al.*, 2005].
[l]Spring snowpack from the Canadian Arctic Archipelago in May (medians), first and second year snow [*St Louis et al.*, 2007].
[m]Spring snowpack from the Canadian Arctic Archipelago in June [*Poulain et al.*, 2007].
[n]Spring snowpack from the Central Basin collected in February to May [*Lu et al.*, 2001].
[o]Supraglacial runoff from the Canadian Arctic Archipelago collected in June and July [*St Louis et al.*, 2005].
[p]Supraglacial runoff from Baffin Bay collected in June [*Zdanowicz et al.*, 2013].
[q]Subglacial runoff from the Canadian Arctic Archipelago collected in June and July [*St Louis et al.*, 2005].
[r]Mackenzie River Canada in June to August [Graydon et al., 2009].
[s]Mackenzie River Canada ice-free season [*Emmerton et al.*, 2013].
[t]Mackenzie River Canada [Leitch et al., 2007].
[u]Mackenzie River and Horton River, Canada in open water (means) [Wang et al., 2012].
[v]Baffin Bay, Canada in June [Zdanowicz et al., 2013].
[w]Zackenberg, Greenland in May to October [Riget et al., 2011a].
[x]Mackenzie, Lena, Ob, Yenisei, and Kolyma rivers [*Amos et al.*, 2014].
[y]Coastal erosion along the Beaufort Sea coast [*Leitch*, 2006].
[z]MeHg fraction of inorganic Hg is assumed to be equal to that found in estuarine and marine surface sediments [Hollweg et al., 2010].

North Atlantic and North Pacific, river discharge, precipitation, and evapotranspiration [Beszczynska-Moller et al., 2012; Curry et al., 2011; Panteleev et al., 2006; Serreze et al., 2006; *Smedsrud et al.*, 2010]. Internal circulation is based on *Alfimov et al.* [2006].

We adapted the solids budget from *Rachold et al.* [2004] to include enhanced productivity with reduced sea ice cover in recent years [Hill et al., 2013]. Productivity (550 Tg C a^{-1}) is distributed equally between the PML and subsurface chlorophyll max [*Arrigo et al.*, 2011]. Settling of suspended particles is based on the fraction of solids

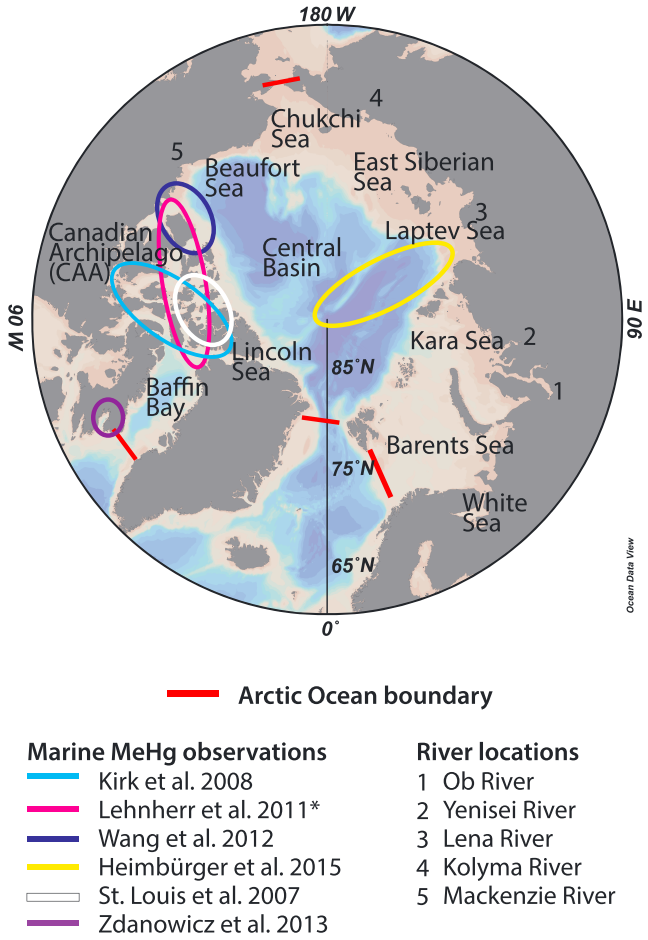

Figure 1. Recent cruises including Hg species measurements in the Arctic Ocean and the Arctic Ocean boundary used in this work. Asterisk represents new data from the same area described in the supporting information Text S2.

remaining following remineralization at each depth in the water column [*Cai et al.*, 2010; *Moran et al.*, 1997; *Rachold et al.*, 2004]. We do not estimate solids resuspension from benthic sediment due to limited data. Burial rates for benthic sediment are based on shelf and deep Central Arctic Basin measurements (Table 3).

2.2. Mercury Reservoirs

We synthesized all data collected since 2004 on Hg species concentrations in seawater (Figure 1), sediment, ice, and biota to estimate reservoirs of Hg species in the Arctic Ocean (Tables 1 and 2). Volumes used to calculate reservoirs are provided in Table 3. Maximum reservoirs of MeHg in primary producers and zooplankton occur in the Arctic summer and are estimated from peak biomass, reservoirs of carbon (g C m^{-2}), and Hg concentrations (Table 3). For phytoplankton and bacteria we used Hg concentrations in seston ($<$200 μm; living organisms and nonliving matter) as a proxy (Table 2) and for zooplankton ($>$200 μm) we estimate mean MeHg burden from Arctic observations (Table S2). Plankton and bacteria reservoirs are not part of the dynamical model and are estimated as a total reservoir for the upper 200 m of the water column.

2.3. Mercury Fluxes

Atmospheric Hg fluxes include direct deposition to ice-free ocean surface waters, a delayed pulse of inputs from seasonal meltwater, and evasion of Hg^0 and Me_2Hg from the surface ocean. We adopt the recent Hg^0 evasion estimate of *Zhang et al.* [2015] that matches observational constraints from atmospheric monitoring data and take leads and ice rafting into account. Evasion of Me_2Hg from ice-free surface waters of 14 Mg a^{-1} is based on the concentration gradient between the PML (Table 1) and marine boundary layer (Table 2), and mean wind speed over the Arctic Ocean (Table 3). Additional details are provided in the supporting information (Table S9).

Direct atmospheric deposition of inorganic Hg to the ice-free surface ocean (Table 3) is taken from recent modeling estimates using the GEOS-Chem global Hg model for consistency with the evasion flux [*Fisher et al.*, 2013; *Zhang et al.*, 2015]. Me_2Hg and MeHg have an atmospheric lifetime of only a few days against decomposition and photodegradation, allowing transport to nearby regions and rapid deposition when Me_2Hg is converted to the more water soluble MeHg [*Bittrich et al.*, 2011; *Lin and Pehkonen*, 1999]. This allows MeHg to be scavenged in precipitation or dry deposit to the ocean and adjacent terrestrial ecosystems before degradation [*St Pierre et al.*, 2015].

There are no direct measurements of MeHg deposition over the Arctic Ocean, so we base atmospheric MeHg deposition (8 Mg a^{-1}) on the evaded Me_2Hg flux and the seasonal fraction of the surface ocean that is ice free (Table 3 and S3). Measured MeHg concentrations in Arctic precipitation (snow and rain) account for $<$0.5 Mg a^{-1} of this flux (Table 4), while the dry deposition flux, calculated using the Hg^{II} dry deposition velocity for water surfaces as a proxy for MeHg [*Baya et al.*, 2015] (Table 3), accounts for between 1 and 5 Mg a^{-1}. Deposition of MeHg with ice crystals (spring) or fog (summer) provides another plausible pathway for enhanced deposition of water-soluble gases (including Hg) [*Douglas et al.*, 2005; *Evenset et al.*, 2004; *Poulain et al.*, 2007; *Rice and Chernyak*, 1997]. Presently, no direct measurements of MeHg concentrations in Arctic fog droplets are available. However, at lower latitude concentrations (17 ± 19 p*M*) up to 2 orders of magnitude higher than oceanic precipitation have been observed [*Weiss-Penzias et al.*, 2012].

We use the average of two model estimates for snowmelt release of inorganic Hg [*Dastoor and Durnford*, 2014; *Fisher et al.*, 2012]. For MeHg, the snowmelt flux is based on the volume of snow deposited to the ice-covered surface ocean and mean concentrations in aged snow and snow melt (Table 4). Hg and MeHg inputs from melting of multiyear sea ice are taken from *Beattie et al.* [2014].

We use inputs of inorganic Hg from Arctic rivers based on terrestrial dissolved organic carbon (DOC) inputs to the ocean from *Dastoor and Durnford* [2014]. This estimate (50 Mg a^{-1}) is slightly larger that the upper bound from a compilation of empirical measurements from *Amos et al.* [2014], which includes new data from Russian rivers. High-resolution data are needed to accurately characterize freshwater discharges of Hg species, and even with new measurements data availability is limited, particularly in the Russian Arctic. Recent work by *Zhang et al.* [2015] based on atmospheric constraints (62 Mg a^{-1}) agrees well with the estimates of *Dastoor and Durnford* [2014]. Inputs of MeHg from rivers are calculated from the observed fraction of total Hg (1–10%, Table 4). The coastal erosion flux of inorganic Hg is based on the solids budget (Figure S1A) and Hg concentrations in eroding material (61–114 ng g^{-1}) from *Leitch* [2006]. The MeHg fraction of total Hg is assumed to be equal to that found in estuarine and marine surface sediments (0.5–2%) [*Hollweg et al.*, 2010] and is set to 1%.

Advective transport of Hg species with inflowing/outflowing seawater and ice is based on flow volumes and measured concentrations at the appropriate flow depths (Figure S1b). Internal transport of Hg species associated with seawater flow among boxes is based on the hydrologic budget (Figure S1B). The surface ocean is strongly stratified [*Macdonald et al.*, 2005], so we only consider vertical Hg fluxes in the PML associated with settling of suspended particles and diffusive transport. We estimate settling rates and burial of Hg species based on the solids budget and Hg concentration data from Table 2.

Within the water column, the eddy diffusion flux is based on concentration gradients between the base of the PML (20 m), the average middepth peak (140 m) and the deep ocean (300 m) [*Heimbürger et al.*, 2015], and the eddy diffusivity. The diffusivity within the Arctic Ocean is highly variable (range <0.01–2.5×10^{-4} m^2 s^{-1}), and we use a mean diffusivity of 0.8×10^{-4} m^2 s^{-1} [*Padman and Dillon*, 1991; *Shaw and Stanton*, 2014; *Wallace et al.*, 1987]. For benthic sediment we use data from North Atlantic estuarine and shelf regions to estimate partitioning of Hg^{II} and MeHg between the dissolved and solid phases (log K_d: Hg = 4.0; MeHg = 2.7) [*Hollweg et al.*, 2010; *Schartup et al.*, 2015a; *Sunderland et al.*, 2006]. Dissolved concentrations are used to calculate upper and lower bounds for diffusion of Hg species at the sediment-water interface [*Sunderland et al.*, 2010] (Table S6).

2.4. Biochemical Transformations

We specify the seawater oxidation rate following the parameterization of *Soerensen et al.* [2010] and constrain the reduction rate using the measured Hg^0:Hg^{II} ratio in PML and subsurface seawater along with Hg^0 evasion loss. Internal production and decomposition of MeHg and Me_2Hg in the water column is based on a compilation of rate constants measured in seawater (Table S1). We calculate a base methylation rate for the deep ocean using experimental measurements from dark filtered seawater [*Monperrus et al.*, 2007] to represent regions of the

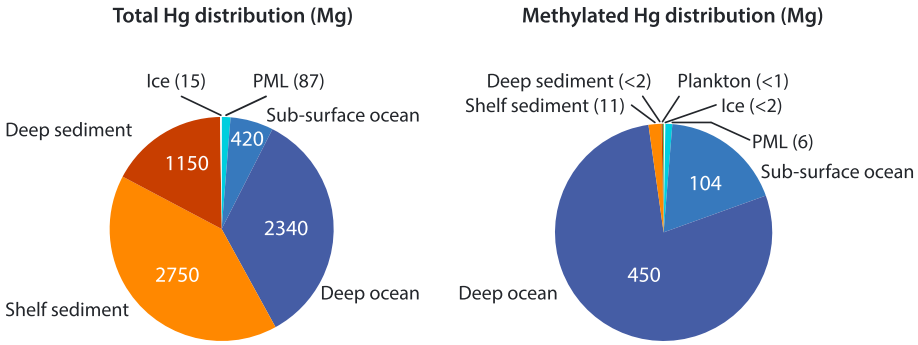

Figure 2. Relative distribution of Hg species reservoirs (Mg) in different components of the Arctic Ocean. MeHg masses in bacteria and plankton fractions are shown in Figure S4.

ocean where remineralization of organic carbon is extremely small. To account for the influence of enhanced microbial activity in the subsurface ocean (20–200 meters) on methylation, we scale the base rate by monthly primary production. Our average methylation rate corresponds to the upper range of experimentally measured values in summer at midlatitudes (0.017 day^{-1}) [*Monperrus et al.*, 2007], and our calculated fall value (0.007 day^{-1}) agrees with rates measured in the Canadian Arctic Archipelago [*Lehnherr et al.*, 2011] (Table S1). No methylation rates have been measured in the Arctic Ocean PML, and we therefore estimate the net biotic methylation needed to close the PML budget for MeHg. This is reasonable given significant, but low, net methylation recently reported in oxic marine waters of the sub-Arctic [*Schartup et al.*, 2015b] and detectable methylation measured at the base of the PML in the Canadian Arctic Archipelago [*Lehnherr et al.*, 2011].

Production of Me_2Hg from MeHg in seawater is taken from direct rate measurements [*Lehnherr et al.*, 2011]. Photolytic MeHg degradation to Hg^{II} in seawater is based on the mean of published rates (Table S1) and averaged summer photosynthetically active radiation (PAR) within the photic zone of ice-free surface waters and melt ponds [*Porter et al.*, 2011; *Serreze and Barry*, 2005] (Table 3). Parsing the photodemethylation rate into specific UV-A, UV-B, and PAR fractions based on Arctic freshwater studies results in a lower degradation flux [*Lehnherr and St. Louis*, 2009]. Biotic degradation/decomposition of Me_2Hg to MeHg is based on data from the deep Pacific Ocean [*Mason et al.*, 1995]. *Black et al.* [2009] did not detect photodegradation of Me_2Hg in the ocean; however, their detection limit was comparable to detected rates of MeHg demethylation (1×10^{-3} E^{-1} m^2) and other studies suggest that photodegradation of Me_2Hg does take place [*Mason and Sullivan*, 1999]. We therefore use a photodegradation rate constant for Me_2Hg of 50% of the detection limit in the *Black et al.* [2009] study. We constrain the reservoir of MeHg available for demethylation using the measured ratio of $MeHg:Hg^{II}$ in seawater.

Methylation in benthic sediment (0.03 day^{-1}) is based on measurements from the North Atlantic shelf and estuaries [*Heyes et al.*, 2006; *Hollweg et al.*, 2010]. The benthic sediment demethylation rate is constrained using the fraction of total Hg as MeHg in porewater (Table S6).

3. Results and Discussion

3.1. Total Hg Budget

Figure 2 shows that more than half of the Hg reservoir in the Arctic Ocean is contained in the active layers of benthic shelf and deep ocean sediment (3900 Mg) followed by an additional 35% in the deep ocean and only 7% in the upper ocean. We estimate that the total Hg reservoir in Arctic seawater is 2870 Mg and has a lifetime against losses of 13 years. The lifetime of total Hg in deep water (>200 m) is longer (45 years) but is still less than deep central Arctic basin tracer ages, which can exceed several hundred years [*Tanhua et al.*, 2009]. This reflects a shorter ventilation time of upper intermediate waters in Baffin Bay and the Barents Sea, which are included in the "deep" model reservoir > 200 m depth. Evasion of gaseous Hg ($Hg^0 + Me_2Hg$: 99 Mg a^{-1}) is the major removal pathway from the water column, accounting for 44% of total losses (Figure 3). Removal of total Hg through seawater outflow to the North Atlantic is 86 Mg a^{-1} (38% of total losses), and sedimentation of suspended solids is relatively smaller at 38 Mg a^{-1} (17% of total losses).

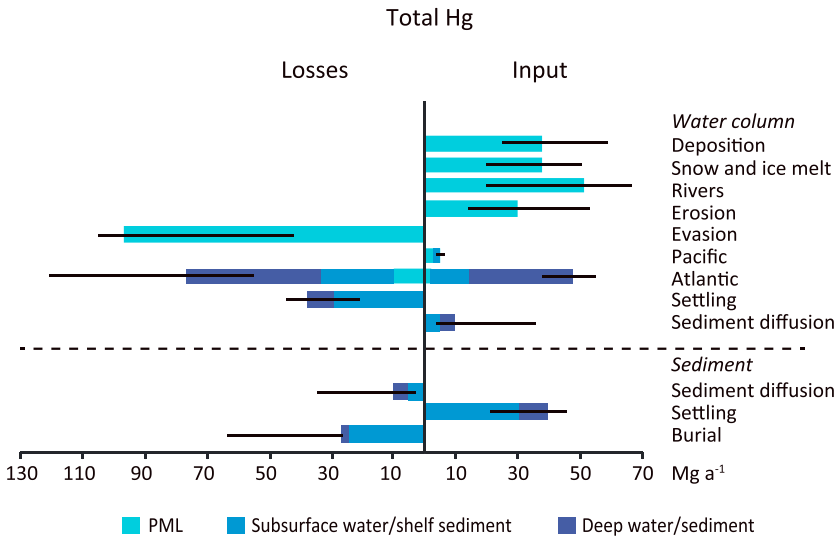

Figure 3. Inputs and losses (Mg a^{-1}) including uncertainty ranges for total Hg. Each ocean depth is indicated by a different color on the plot. Inputs and losses through water exchange with the Atlantic Ocean are shown as gross fluxes.

Figure 3 shows that the terrestrial environment accounts for more than a third of total Hg inputs to the water column (erosion and rivers: 84 Mg a^{-1}), as does the atmosphere (direct deposition and meltwater: 76 Mg a^{-1}). Ocean inflow from the North Atlantic and North Pacific account for an additional 53 Mg a^{-1} (24%), and sediment diffusion makes up the remaining 5% of total inputs (11 Mg a^{-1}). High gaseous Hg ($Hg^0 + Me_2Hg$) evasion (99 Mg a^{-1}) is driven by substantial inputs of total Hg from rivers and coastal erosion and declining sea ice cover [*Chen et al.*, 2015; *Zhang et al.*, 2015]. The difference between evasion and inputs from meltwater and direct atmospheric deposition of total Hg in our budget (−23 Mg a^{-1}) suggests that the Arctic Ocean is a net source to the atmosphere, which is consistent with previous work [*Fisher et al.*, 2012; *Sonke and Heimbürger*, 2012; *Zhang et al.*, 2015].

Figure 4 shows that Arctic seawater is enriched in total Hg relative to inflowing waters from the North Atlantic and North Pacific Oceans at all depths resulting in a 26 Mg a^{-1} net loss from the Arctic via circulation. We infer from our mass budget that the observed enrichment in total Hg in Arctic seawater relative to midlatitude basins is caused by higher freshwater inputs relative to basin size and inhibition of losses through Hg^0 evasion due to ice cover. Future increases in mobilization of Hg from thawing permafrost [*Leitch*, 2006; *Rydberg et al.*, 2010] could increase Hg inputs to the Arctic Ocean, offsetting the current declining trend due to enhanced losses from Hg^0 evasion with sea ice retreat suggested in earlier work [*Chen et al.*, 2015; *Fisher et al.*, 2013].

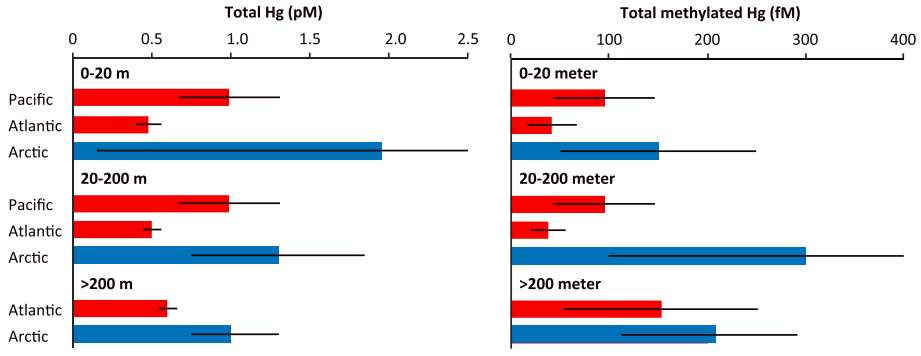

Figure 4. Total Hg and methylated Hg concentrations in seawater flowing into (red) and out of (blue) the Arctic Ocean. Atlantic Ocean concentrations for each depth interval are based on 2013 measurements in the North Atlantic (50°N–62°N) (supporting information Text S1). Pacific Ocean concentrations are from the upper 50 m of the water column close to the shallow sill at the Bering Strait [*Sunderland et al.*, 2009]. We use Hg species concentrations in seawater and ice leaving the Arctic through the Barents Sea, Fram Strait, and Davis Strait (Table 1).

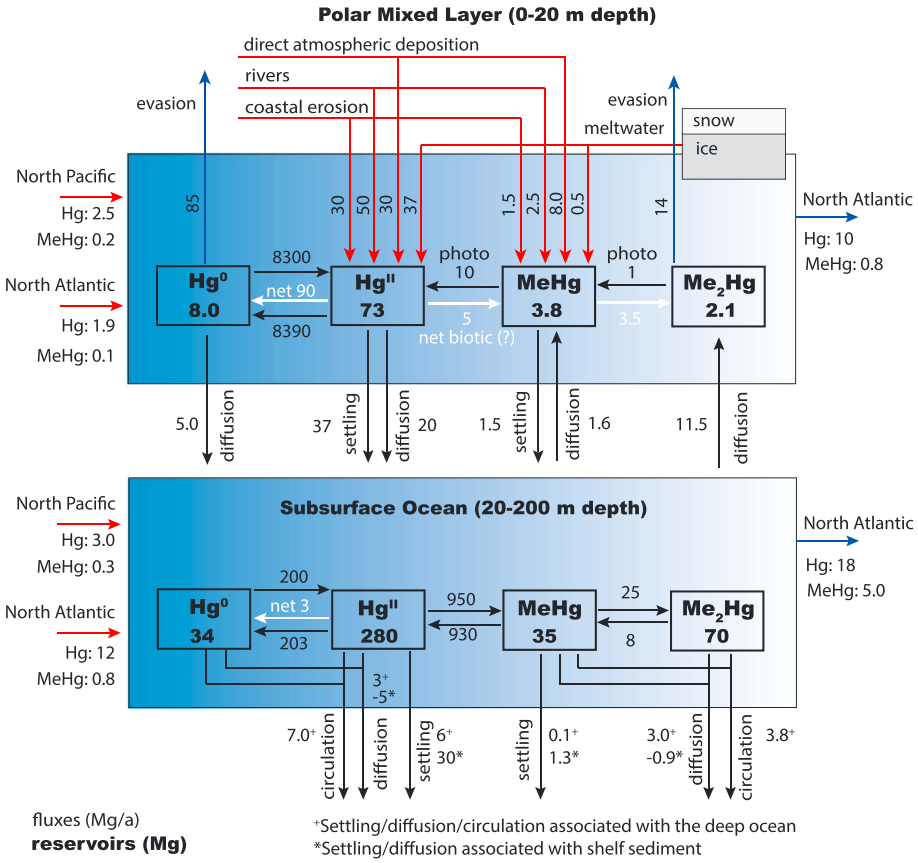

Figure 5. Reservoirs (Mg) and mass flows (Mg a^{-1}) in the Arctic polar mixed layer (PML) and subsurface ocean. Red arrows indicate external sources, blue arrows denote losses out of the system, black arrows show internal fluxes, and white arrows indicate net fluxes. Figure 3 shows fluxes for the deep ocean, which cannot be resolved on species-specific basis due to lack of data.

3.2. Methylated Hg Species Budget

The stability of MeHg and Me_2Hg is enhanced in the dark, cold conditions with low biological activity found in the deep ocean. This reservoir contains almost 80% of the methylated species (450 Mg) in the Arctic Ocean (Figure 2). However, the PML and subsurface ocean are the most important reservoirs for MeHg accumulation at the base of the food web due to the concentration of algal production and biological foraging in these regions. Summer peak concentrations of MeHg in phytoplankton and zooplankton indicate a reservoir of only 0.7 Mg or about 2% of the MeHg reservoir in the upper ocean (0–200 m) (Figure 2).

Unlike total Hg, only a small fraction of methylated Hg species are found in benthic sediment (2.2%) (Figure 2), and we do not calculate a substantial diffusive flux from benthic sediments to the overlying water column (<1 Mg a^{-1}). Data on Arctic-wide solids resuspension are needed to further elucidate on the importance of sediments as a MeHg source to the shelf water column.

Similar to total Hg, methylated Hg species are enriched in the Arctic Ocean at all depths relative to inflowing seawater from the North Atlantic and North Pacific Oceans and subsurface waters have a MeHg:total Hg ratio double that of inflowing water (Figure 4). For methylated Hg species, peak concentrations in excess of 200 fM are found in subsurface seawater (20–200 m). Subsurface seawater peaks in concentrations of methylated Hg species are observable across the global oceans [*Bowman et al.*, 2015; *Cossa et al.*, 2011; *Sunderland et al.*, 2009] but occur at much shallower depths in the Arctic [*Heimbürger et al.*, 2015; *Lehnherr et al.*, 2011]. A smaller fraction of methylated Hg is present as Me_2Hg in the PML compared to subsurface seawater, while MeHg concentrations are similar in the two layers (Table 1). Evasion of Me_2Hg from the PML may partially explain the subsurface peak in methylated Hg. Enhanced methylation in relatively shallow waters due to the pronounced halocline structure of the Arctic is likely also an important factor [*Heimbürger et al.*, 2015; *Schartup et al.*, 2015b]. For example,

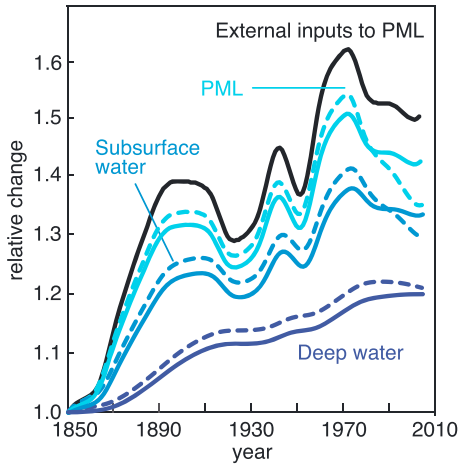

Figure 6. Modeled temporal trajectory of total Hg concentrations in Arctic Ocean seawater in response to changes in atmospheric Hg loading since 1850 and 1975–present declines in sea ice cover. Sea ice retreat is modeled assuming a 15% linear decrease between 1975 and 2010 based on annual sea ice data from *AMAP* [2011b].The solid black line denotes changes in total inputs to the polar mixed layer (PML) calculated by scaling present-day Arctic atmospheric inputs (including snowmelt) by historical deposition trends from *Horowitz et al.* [2014] based on shifts in global emissions. Ocean water column responses are shown by the blue lines. The solid line represents a scenario forced only by atmospheric inputs (constant present-day sea ice), and the dashed line considers the impact of both changing inputs and sea ice retreat since 1975.

salinity-driven stratification can concentrate terrestrial dissolved organic matter (DOM) in a relatively restricted vertical zone. Terrestrial DOM stimulates the activity of methylating bacteria in estuaries, increasing MeHg production [*Schartup et al.*, 2015b]. Climate driven increases in stratification of Arctic seawater and declining sea ice cover, and age may thus have a large impact on future levels of methylated Hg production and loss.

Figure 5 shows that net production of MeHg from Hg^{II} only occurs in the water column of the subsurface (20–200 m depth) ocean (20 Mg a^{-1}). A large fraction of MeHg produced in the subsurface ocean is converted to Me_2Hg (17 Mg a^{-1}), much of which diffuses to the PML (~12 Mg a^{-1}) and is evaded to the atmosphere (14 Mg a^{-1}). Our budget suggests the major net source of MeHg to the PML is atmospheric redeposition of this evaded Me_2Hg (~8 Mg a^{-1}) originally produced in the subsurface ocean. This supposition is supported by findings of elevated MeHg concentrations in the terrestrial landscape near sea ice leads but requires confirmation with direct measurements [*St Pierre et al.*, 2015].

In addition to deposition, MeHg sources to the PML include rivers (2.5 Mg a^{-1}), diffusion from the subsurface ocean (1.6 Mg a^{-1}), erosion (1.5 Mg a^{-1}), photolytic and biotic degradation of Me_2Hg in the water column (1.5 Mg a^{-1}), and inflow from the North Atlantic and Pacific (0.3 Mg a^{-1}). The reservoir of MeHg in the PML is small (3.8 Mg) and turnover is relatively fast (Figure 5). Thus, we assume on an annual basis the MeHg budget must balance and infer based on this assumption that a small net biotic production of MeHg in the range of other inputs occurs in the PML water column (5 Mg a^{-1}). *Lehnherr et al.* [2011] observed significant methylation at the base of the PML in the Canadian Arctic Archipelago, and *Schartup et al.* [2015b] measured net dark methylation in oxic estuarine seawater from the sub-Arctic. Both studies indicate that net biotic methylation in the PML is plausible.

3.3. Response to Global Change and Anthropogenic Emissions

Biogeochemical cycling of Hg in the Arctic Ocean is highly sensitive to ongoing climate variability [*Fisher et al.*, 2013; *Krabbenhoft and Sunderland*, 2013; *Stern et al.*, 2012]. Mean air temperature is increasing rapidly, driving decreases in the extent and thickness of sea ice cover [*Bintanja et al.*, 2011; *Kwok and Rothrock*, 2009]. In addition, changes in the magnitude and spatial distribution of global anthropogenic Hg emissions affect atmospheric inputs to the Arctic Ocean, both directly through deposition to the ocean and indirectly through terrestrial runoff [*Stern et al.*, 2012].

Figure 6 illustrates the timescales of response to changes in the Arctic. Our modeled changes in total Hg in Arctic Ocean seawater are forced by differences in direct atmospheric inputs and changes in sea ice cover. Atmospheric inputs since 1850 are estimated by scaling current inputs using historical deposition scenarios from *Horowitz et al.* [2014]. We assume a 4.3% decrease per decade in sea ice since 1975 based on the data from AMAP (total of 15% decrease from 1975 to 2010) [*AMAP*, 2011b]. Modeled inputs from all external sources to the PML increased by 50% between 1850 and 2010 and have an almost linear effect on total Hg

concentrations in the PML (44%) and subsurface water (33%) (Figure 6) reflecting the short turnover time of the total Hg reservoir in the upper ocean (~3 year for 0–200 m; Figure 5). *Outridge et al.* [2008] hypothesized that MeHg concentrations in the Arctic Ocean are unlikely to be affected by changes in external Hg inputs due to the large inorganic Hg reservoir, which they suggested provides inertia against changes in loading over time. Our simulations illustrate that for the most biologically relevant parts of the water column (0–200 m), regulatory actions that decrease Hg emission and associated atmospheric deposition have the capacity to rapidly affect aquatic Hg concentrations.

Concentrations of methylated Hg can be expected to follow changes in inorganic Hg relatively quickly given the rapid turnover of the methylated Hg reservoirs and first-order nature of reactions [*Benoit et al.*, 2003; *Ullrich et al.*, 2001]. The impacts of changes in Hg loading may be obscured by other biogeochemical shifts in the ecosystem affecting the bioavailable MeHg fraction, losses through evasion, and relative balance between methylation and demethylation reactions. Isolating the potential influence of anthropogenic emissions and sea ice melt allows us to diagnose their relative importance for future change, although a comprehensive analysis of all simultaneously occurring factors is not yet possible. For example, Figure 6 suggests that a decline in sea ice in recent years results in a net loss of oceanic Hg due to increased evasion [*Chen et al.*, 2015].

Ongoing changes in the terrestrial landscape such as permafrost melt and increases in freshwater discharges of DOM are likely to increase MeHg inputs from Arctic rivers to the ocean in the future but remain a critical uncertainty in our analysis as data are presently inadequate to quantify such processes across the Arctic [*Krabbenhoft and Sunderland*, 2013; *Rydberg et al.*, 2010]. The relative importance of external MeHg sources to the Arctic Ocean depends in large part on the stability of MeHg complexes in seawater, and this can also affect our estimated lifetime in seawater. Recent work by *Jonsson et al.* [2014] suggests that riverine MeHg bound to terrestrial DOM is both resistant to degradation and biologically available. Thus, the overall lifetime of MeHg in the ocean is likely to be enhanced in the future with increasing terrestrial DOM discharges, which would lead to increases in the MeHg reservoir.

4. Summary and Conclusion

We have developed a five-box biogeochemical model for the Arctic Ocean to gain insight into processes and timescales driving changes in MeHg concentrations in the Arctic Ocean. The model includes compartments representing three ocean and two sediment reservoirs: the PML, subsurface and deep ocean water, and active sediment layers on the shelf and in the Central Basin.

Results from the total Hg mass budget calculations suggest that exchange with both the atmosphere (including snowmelt) and lower latitude ocean results in net loss of total Hg from the Arctic Ocean. The terrestrial landscape is the only net Hg source. We use the box model simulation to demonstrate the importance of the sea ice cover in controlling surface ocean evasion loss. From this we infer that the observed enrichment in total Hg in Arctic seawater relative to midlatitude basins is caused by higher relative freshwater Hg inputs and ice cover that inhibits losses through evasion.

The methylated Hg budget suggests that most net MeHg production (20 Mg a^{-1}) occurs in the subsurface ocean (20–200 m). There it is subsequently converted to Me_2Hg (17 Mg a^{-1}), which readily diffuses to the PML and is evaded to the atmosphere (14 Mg a^{-1}). Me_2Hg has an atmospheric lifetime of only a few days and rapidly photochemically degrades back to MeHg. We hypothesize that most evaded Me_2Hg is redeposited to the ocean and surrounding landscape as MeHg and that atmospheric MeHg deposition is the largest net source (8 Mg a^{-1}) to the biologically productive surface ocean (0–20 m). We find that other important MeHg sources to the PML are river input (2.5 Mg a^{-1}) and proposed net biotic methylation (5 Mg a^{-1}). Rivers are likely to be disproportionately important for biological uptake in marine food webs since binding to terrestrial DOM extends the MeHg lifetime in the water column. We suggest that the overall lifetime of MeHg in the Arctic Ocean is likely to be enhanced in the future with increasing terrestrial DOM discharges.

We forced our box model of the Arctic Ocean with changes in sea ice and anthropogenic Hg deposition from 1850 to 2010. Our results show that because of the short lifetime (3 years) of total Hg in the most biologically relevant parts of the water column (0–200 m), regulatory actions that decrease Hg emission and associated atmospheric deposition have the capacity to rapidly affect aquatic Hg concentrations.

4.1. Limitations and Uncertainties

Extensive Hg and MeHg measurements have been collected throughout the Canadian Arctic Archipelago, but only four vertical profiles are presently available from the Central Arctic Basin [*Heimbürger et al.,* 2015]. Our work highlights a particular need for additional speciated mercury measurements in the Central Basin and accompanying water column methylation and demethylation rate measurements. Data synthesized here were insufficient to estimate solids resuspension from benthic sediment, which could be an important source of MeHg to coastal regions. A main hypothesis stemming from this work is that high Me_2Hg concentrations in the PML results in a high evasion flux into the Arctic boundary layer, followed by decomposition to, and deposition of, MeHg. This hypothesis is supported by findings of elevated MeHg concentrations in the marine boundary layer and terrestrial landscape near sea ice leads [*Baya et al.,* 2015; *St Pierre et al.,* 2015], but additional measurements are needed to confirm this process. Another key uncertainty is the magnitude of pan-Arctic Hg and MeHg fluxes in freshwater discharge and the impacts of terrestrial and marine dissolved organic matter on reduction and methylation. Field measurements that fill these important gaps will help refine the pan-Arctic budgets for Hg and MeHg presented here.

Acknowledgments

We acknowledge financial support from the U.S. National Science Foundation (OCE 1130549, PLR 1023213). A.L.S. acknowledges financial support from the Carlsberg Foundation. J.A.F. acknowledges financial support from the University of Wollongong Vice Chancellor's Postdoctoral Fellowship. J. E.S. acknowledges financial support from the European Research Council (ERC-2010-StG_20091028). I.L. and V.S.L. acknowledge financial support from the Northern Contaminants Program and ArcticNet. Supporting data are included as nine tables, four figures, and two sections of text in a supporting information file.

References

Alfimov, V., G. Possnert, and A. Aldahan (2006), Anthropogenic iodine-129 in the Arctic Ocean and Nordic Seas: Numerical modeling and prognoses, *Mar. Pollut. Bull.*, *52*(4), 380–385.

Arctic Monitoring and Assessment Programme (AMAP) (2011a), AMAP Assessment 2011: Mercury in the Arctic. Arctic Monitoring and Assessment Programme (AMAP), *Rep.*, xiv + 193 pp., Oslo, Norway.

Arctic Monitoring and Assessment Programme (AMAP) (2011b), Snow, Water, Ice and Permafrost in the Arctic (SWIPA): Climate change and the cryosphere. Arctic Monitoring and Assessment Programme (AMAP), *Rep.*, 538 pp., Oslo, Norway.

Amos, H. M., D. J. Jacob, D. Kochman, H. M. Horowitz, Y. Zhang, S. Dutkiewicz, M. Horvat, E. S. Corbitt, and E. M. Sunderland (2014), Global biogeochemical implications of mercury discharges from tivers and sediment burial, *Environ. Sci. Technol.*, *48*(16), 9514–9522, doi:10.1021/es502134t.

Andersson, M. E., J. Sommar, K. Gardfeldt, and O. Lindqvist (2008), Enhanced concentrations of dissolved gaseous mercury in the surface waters of the Arctic Ocean, *Mar. Chem.*, *110*(3–4), 190–194.

Arrigo, K. R., and G. L. van Dijken (2011), Secular trends in Arctic Ocean net primary production, *J. Geophys. Res.*, *116*, C09011, doi:10.1029/2011JC007151.

Arrigo, K. R., P. A. Matrai, and G. L. van Dijken (2011), Primary productivity in the Arctic Ocean: Impacts of complex optical properties and subsurface chlorophyll maxima on large-scale estimates, *J. Geophys. Res.*, *116*, C11022, doi:10.1029/2011JC007273

Baya, P. A., M. Gosselin, I. Lehnherr, V. L. St. Louis, and H. Hintelmann (2015), Determination of monomethylmercury and dimethylmercury in the Arctic marine boundary layer, *Environ. Sci. Technol.*, *49*(1), 223–232, doi:10.1021/es502601z.

Beattie, S. A., D. Armstrong, A. Chaulk, J. Comte, M. Gosselin, and F. Y. Wang (2014), Total and methylated mercury in Arctic multiyear sea ice, *Environ. Sci. Technol.*, *48*(10), 5575–5582.

Benoit, J., C. Gilmour, A. Heyes, R. Mason, and C. Miller (2003), *Geochemical and Biological Controls Over Methylmercury Production and Degradation in Aquatic Ecosystems, ACS Symposium Series*, vol. 835, Am. Chem. Soc., Washington, D. C., 1999.

Beszczynska-Moller, A., E. Fahrbach, U. Schauer, and E. Hansen (2012), Variability in Atlantic water temperature and transport at the entrance to the Arctic Ocean, 1997–2010, *ICES J. Mar. Sci.*, *69*(5), 852–863.

Bintanja, R., R. G. Graversen, and W. Hazeleger (2011), Arctic winter warming amplified by the thermal inversion and consequent low infrared cooling to space, *Nat. Geosci.*, *4*(11), 758–761, doi:10.1038/ngeo1285.

Bittrich, D. R., A. P. Rutter, B. D. Hall, and J. J. Schauer (2011), Photodecomposition of methylmercury in atmospheric waters, *Aerosol and Air Qual. Res.*, *11*(3), 290–299.

Black, F. J., C. H. Conaway, and A. R. Flegal (2009), Stability of dimethyl mercury in seawater and its conversion to monomethyl mercury, *Environ. Sci. Technol.*, *43*(11), 4056–4062.

Bowman, K. L., C. R. Hammerschmidt, C. H. Lamborg, and G. Swarr (2015), Mercury in the North Atlantic Ocean: The U.S. GEOTRACES zonal and meridional sections, *Deep Sea Res., Part II*, doi:10.1016/j.dsr2.2014.07.004.

Braune, B., et al. (2015), Mercury in the marine environment of the Canadian Arctic: Review of recent findings, *Sci. Total Environ.*, *509*, 67–90, doi:10.1016/j.scitotenv.2014.05.133.

Burt, A. E. (2012), Mercury uptake and dynamics in sea ice algae, phytoplankton and grazing copepods from a Beaufort Sea Arctic marine food web, 92 pp., Univ. of Manitoba. [Available at http://hdl.handle.net/1993/8907.]

Cai, P., M. R. van der Loeff, I. Stimac, E. M. Nothig, K. Lepore, and S. B. Moran (2010), Low export flux of particulate organic carbon in the central Arctic Ocean as revealed by Th-234:U-238 disequilibrium, *J. Geophys. Res.*, *115*, C10037, doi:10.1029/2009JC005595

Canario, J., L. Poissant, M. Pilote, C. Blaise, P. Constant, J.-F. Ferard, and F. Gagne (2013), Toxicity survey of Canadian Arctic marine sediments, *J. Soils Sediments*, *14*, 196–203, doi:10.1007/s11368-013-0792-1.

Chaulk, A., G. A. Stern, D. Armstrong, D. G. Barber, and F. Y. Wang (2011), Mercury distribution and transport across the ocean-sea-ice-atmosphere interface in the Arctic Ocean, *Environ. Sci. Technol.*, *45*(5), 1866–1872.

Chen, L., Y. Zhang, D. J. Jacob, A. Soerensen, J. A. Fisher, H. M. Horowitz, E. S. Corbitt, and X. Wang (2015), Differences in decadal trends of atmospheric mercury between the Arctic and northern mid-latitudes suggest a decline in Arctic Ocean mercury, *Geophys. Res. Lett.*, *42*, 6076–6083, doi:10.1002/2015GL064051.

Clough, L. M., W. G. Ambrose, J. K. Cochran, C. Barnes, P. E. Renaud, and R. C. Aller (1997), Infaunal density, biomass and bioturbation in the sediments of the Arctic Ocean, *Deep Sea Res., Part II*, *44*(8), 1683–1704.

Cossa, D., L. E. Heimbürger, D. Lannuzel, S. R. Rintoul, E. C. V. Butler, A. R. Bowie, B. Averty, R. J. Watson, and T. Remenyi (2011), Mercury in the Southern Ocean, *Geochim. Cosmochim. Acta*, *75*(14), 4037–4052, doi:10.1016/j.gca.2011.05.001.

Curry, B., C. M. Lee, and B. Petrie (2011), Volume, freshwater, and heat fluxes through Davis Strait, 2004–05, *J. Phys. Oceanogr.*, *41*(3), 429–436.

Dastoor, A., and D. Durnford (2014), Arctic Ocean: Is it a sink or a source of atmospheric mercury?, *Environ. Sci. Technol.*, *48*(3), 1707–1717, doi:10.1021/es404473e.
Dastoor, A., A. Ryzhkov, D. Durnford, I. Lehnherr, A. Steffen, and H. Morrison (2015), Atmospheric mercury in the Canadian Arctic. Part II: Insight from modeling, *Sci. Total Environ.*, *509*, 16–27.
Dittmar, T., and G. Kattner (2003), The biogeochemistry of the river and shelf ecosystem of the Arctic Ocean: A review, *Mar. Chem.*, *83*(3–4), 103–120.
Douglas, T., M. Sturm, W. Simpson, S. Brooks, S. Lindberg, and D. Perovich (2005), Elevated mercury measured in snow and frost flowers near Arctic sea ice leads, *Geophys. Res. Lett.*, *32*, L04502, doi:10.1029/2004GL022132.
Emmerton, C. A., J. A. Graydon, J. A. L. Gareis, V. L. St. Louis, L. F. W. Lesack, J. K. A. Banack, F. Hicks, and J. Nafziger (2013), Mercury export to the Arctic Ocean from the Mackenzie River, Canada, *Environ. Sci. Technol.*, doi:10.1021/es400715r.
Evenset, A., G. N. Christensen, T. Skotvold, E. Fjeld, M. Schlabach, E. Wartena, and D. Gregor (2004), A comparison of organic contaminants in two high Arctic lake ecosystems, Bjornoya (Bear Island), Norway, *Sci. Total Environ.*, *318*(1–3), 125–141.
Fisher, J. A., D. J. Jacob, A. L. Soerensen, H. M. Amos, A. Steffen, and E. M. Sunderland (2012), Riverine source of Arctic Ocean mercury inferred from atmospheric observations, *Nat. Geosci.*, *5*(7), 499–504.
Fisher, J. A., D. J. Jacob, A. L. Soerensen, H. M. Amos, E. S. Corbitt, D. G. Streets, Q. Wang, R. M. Yantosca, and E. M. Sunderland (2013), Factors driving mercury variability in the Arctic atmosphere and ocean over the past thirty years, *Global Biogeochem. Cycles*, *27*, 1226–1235, doi:10.1002/2013GB004689.
Fox, A. L., E. A. Hughes, R. P. Trocine, J. H. Trefry, S. V. Schonberg, N. D. McTigue, B. K. Lasorsa, B. Konar, and L. W. Cooper (2013), Mercury in the northeastern Chukchi Sea: Distribution patterns in seawater and sediments and biomagnification in the benthic food web, *Deep Sea Res., Part II*, doi:10.1016/j.dsr2.2013.07.012.
Galand, P. E., C. Lovejoy, J. Pouliot, and W. F. Vincent (2008), Heterogeneous archaeal communities in the particle-rich environment of an arctic shelf ecosystem, *J. Mar. Sys.*, *74*(3–4), 774–782, doi:10.1016/j.jmarsys.2007.12.001.
Graydon, J. A., C. A. Emmerton, L. F. W. Lesack, and E. N. Kelly (2009), Mercury in the Mackenzie River delta and estuary: Concentrations and fluxes during open-water conditions, *Sci. Total Environ.*, *407*(8), 2980–2988.
Hammerschmidt, C. R., W. F. Fitzgerald, C. H. Lamborg, P. H. Balcom, and C. M. Tseng (2006), Biogeochemical cycling of methylmercury in lakes and tundra watersheds of Arctic Alaska, *Environ. Sci. Technol.*, *40*(4), 1204–1211.
Hansell, D. A., C. A. Carlson, and R. Schlitzer (2012), Net removal of major marine dissolved organic carbon fractions in the subsurface ocean, *Global Biogeochem. Cycles*, *26*, GB1016, doi:10.1029/2011GB004069.
Hatzianastassiou, N., C. Matsoukas, A. Fotiadi, K. G. Pavlakis, E. Drakakis, D. Hatzidimitriou, and I. Vardavas (2005), Global distribution of Earth's surface shortwave radiation budget, *Atmos. Chem. Phys.*, *5*, 2847–2867.
Hedges, J. I., J. A. Baldock, Y. Gelinas, C. Lee, M. L. Peterson, and S. G. Wakeham (2002), The biochemical and elemental compositions of marine plankton: A NMR perspective, *Mar. Chem.*, *78*(1), 47–63.
Heimbürger, L. E., J. Sonke, D. Cossa, D. Point, C. Lagane, L. Laffont, B. Galfond, M. Nicolaus, B. Rabe, and M. M. Rutgers van der Loeff (2015), Shallow methylmercury production in the marginal sea ice zone of the central Arctic Ocean, *Sci. Rep.*, *5*, doi:10.1038/srep10318.
Heyes, A., R. P. Mason, E. H. Kim, and E. Sunderland (2006), Mercury methylation in estuaries: Insights from using measuring rates using stable mercury isotopes, *Mar. Chem.*, *102*(1–2), 134–147, doi:10.1016/J.Marchem.2005.09.018.
Hill, V. J., P. A. Matrai, E. Olson, S. Suttles, M. Steele, L. A. Codispoti, and R. C. Zimmerman (2013), Synthesis of integrated primary production in the Arctic Ocean: II. In situ and remotely sensed estimates, *Prog. Oceanogr.*, *110*, 107–125.
Hollweg, T. A., C. C. Gilmour, and R. P. Mason (2010), Mercury and methylmercury cycling in sediments of the mid-Atlantic continental shelf and slope, *Limnol. Oceanogr.*, *55*(6), 2703–2722.
Horowitz, H. M., D. J. Jacob, H. M. Amos, D. G. Streets, and E. M. Sunderland (2014), Historical Mercury releases from commercial products: Global environmental implications, *Environ. Sci. Technol.*, *48*(17), 10,242–10,250, doi:10.1021/es501337j.
Horvat, M., J. Kotnik, M. Logar, V. Fajon, T. Zvonaric, and N. Pirrone (2003), Speciation of mercury in surface and deep-sea waters in the Mediterranean Sea, *Atmos. Environ.*, *37*, S93–S108.
Jakobsson, M. (2002), Hypsometry and volume of the Arctic Ocean and its constituent seas, *Geochem. Geophys. Geosyst.*, *3*(2), 1028, doi:10.1029/2001GC000302
Jin, M. B., C. Deal, S. H. Lee, S. Elliott, E. Hunke, M. Maltrud, and N. Jeffery (2012), Investigation of Arctic sea ice and ocean primary production for the period 1992–2007 using a 3-D global ice-ocean ecosystem model, *Deep Sea Res., Part Ii*, *81–84*, 28–35.
Jonsson, S., U. Skyllberg, M. B. Nilsson, E. Lundberg, A. Andersson, and E. Bjorn (2014), Differentiated availability of geochemical mercury pools controls methylmercury levels in estuarine sediment and biota, *Nat. Commun.*, *5*, doi:10.1038/ncomms5624.
Kading, T., and M. Andersson (2011), Mercury and methylmercury distribution in Arctic Ocean sediments, paper presented at the International Conference on Mercury as a Global Pollutant, Halifax, Canada.
Kirchman, D. L., V. Hill, M. T. Cottrell, R. Gradinger, R. R. Malmstrom, and A. Parker (2009), Standing stocks, production, and respiration of phytoplankton and heterotrophic bacteria in the western Arctic Ocean, *Deep Sea Res., Part II*, *56*(17), 1237–1248.
Kirk, J. L., V. L. St. Louis, and M. J. Sharp (2006), Rapid reduction and reemission of mercury deposited into snowpacks during atmospheric mercury depletion events at Churchill, Manitoba, Canada, *Environ. Sci. Technol.*, *40*(24), 7590–7596, doi:10.1021/es061299.
Kirk, J. L., V. L. S. Louis, H. Hintelmann, I. Lehnherr, B. Else, and L. Poissant (2008), Methylated mercury species in marine waters of the Canadian high and sub Arctic, *Environ. Sci. Technol.*, *42*(22), 8367–8373.
Kirk, J. L., et al. (2012), Mercury in Arctic marine ecosystems: Sources, pathways and exposure, *Environ. Res.*, *119*, 64–87.
Kosobokova, K., and H. J. Hirche (2009), Biomass of zooplankton in the eastern Arctic Ocean—A base line study, *Prog. Oceanogr.*, *82*(4), 265–280.
Krabbenhoft, D. P., and E. M. Sunderland (2013), Global change and mercury, *Science*, *341*(6153), 1457–1458.
Kuzyk, Z. Z. A., C. Gobeil, and R. W. Macdonald (2013), ^{210}Pb and ^{13}7Cs in margin sediments of the Arctic Ocean: Controls on boundary scavenging, *Global Biogeochem. Cycles*, *27*, 1–18, doi:10.1002/gbc.20041.
Kwok, R., and D. A. Rothrock (2009), Decline in Arctic sea ice thickness from submarine and ICESat records: 1958–2008, *Geophys. Res. Lett.*, *36*, L15501, doi:10.1029/2009GL039035.
Lalonde, J. D., A. J. Poulain, and M. Amyot (2002), The role of mercury redox reactions in snow on snow-to-air mercury transfer, *Environ. Sci. Technol.*, *36*(2), 174–178, doi:10.1021/es010786g.
Lehnherr, I. (2014), Methylmercury biogeochemistry: A review with special reference to Arctic aquatic ecosystems, *Environ. Rev.*, *22*(3), 229–243, doi:10.1139/er-2013-0059.
Lehnherr, I., and V. L. St. Louis (2009), Importance of ultraviolet radiation in the photodemethylation of methylmercury in freshwater ecosystems, *Environ. Sci. Technol.*, *43*(15), 5692–5698.

Lehnherr, I., V. L. St. Louis, H. Hintelmann, and J. L. Kirk (2011), Methylation of inorganic mercury in polar marine waters, *Nat. Geosci.*, *4*(5), 298–302.
Lehnherr, I., V. L. St. Louis, C. A. Emmerton, J. D. Barker, and J. L. Kirk (2012), Methylmercury cycling in High Arctic wetland ponds: Sources and sinks, *Environ. Sci. Technol.*, *46*(19), 10,514–10,522.
Leitch, D. R. (2006), *Mercury Distribution in Water and Permafrost of the Lower Mackenzie Basin, Their Contribution to the Mercury Contamination in the Beaufort Sea Marine Ecosystem, and Potential Effects of Climate Variation*, pp. 130, Univ. of Manitoba, Winnipeg, Manitoba.
Leitch, D. R., J. Carrie, D. Lean, R. W. Macdonald, G. A. Stern, and F. Y. Wang (2007), The delivery of mercury to the Beaufort Sea of the Arctic Ocean by the Mackenzie River, *Sci. Total Environ.*, *373*(1), 178–195.
Lin, C.-J., and S. O. Pehkonen (1999), The chemistry of atmospheric mercury: A review, *Atmos. Environ.*, *33*(13), 2067–2079.
Lu, J. Y., W. H. Schroeder, L. A. Barrie, A. Steffen, H. E. Welch, K. Martin, L. Lockhart, R. V. Hunt, G. Boila, and A. Richter (2001), Magnification of atmospheric mercury deposition to polar regions in springtime: The link to tropospheric ozone depletion chemistry, *Geophys. Res. Lett.*, *28*(17), 3219–3222, doi:10.1029/2000GL012603.
Macdonald, R. W., T. Harner, and J. Fyfe (2005), Recent climate change in the Arctic and its impact on contaminant pathways and interpretation of temporal trend data, *Sci. Total Environ.*, *342*(1–3), 5–86.
Mason, R. P., and K. A. Sullivan (1999), The distribution and speciation of mercury in the South and equatorial Atlantic, *Deep Sea Res., Part II*, *46*(5), 937–956.
Mason, R. P., K. R. Rolfhus, and W. F. Fitzgerald (1995), Methylated and elemental mercury cycling in surface and deep-ocean waters of the North-Atlantic, *Water Air Soil Pollut.*, *80*(1–4), 665–677.
Mason, R. P., A. L. Choi, W. F. Fitzgerald, C. R. Hammerschmidt, C. H. Lamborg, A. L. Soerensen, and E. M. Sunderland (2012), Mercury biogeochemical cycling in the ocean and policy implications, *Environ. Res.*, *119*, 101–117, doi:10.1016/j.envres.2012.03.013.
Monperrus, M., E. Tessier, D. Amouroux, A. Leynaert, P. Huonnic, and O. F. X. Donard (2007), Mercury methylation, demethylation and reduction rates in coastal and marine surface waters of the Mediterranean Sea, *Mar. Chem.*, *107*(1), 49–63.
Moran, S. B., K. M. Ellis, and J. N. Smith (1997), Th-234/U-238 disequilibrium in the central Arctic Ocean: Implications for particulate organic carbon export, *Deep Sea Res., Part II*, *44*(8), 1593–1606.
Nagorski, S. A., D. R. Engstrom, J. P. Hudson, D. P. Krabbenhoft, E. Hood, J. F. Dewild, and G. R. Aiken (2014), Spatial distribution of mercury in southeastern Alaskan streams influenced by glaciers, wetland, and salmon, *Environ. Pollut.*, *184*, 62–72, doi:10.1016/j.envpol.2013.07.040.
National Snow and Ice Data Center (NSIDC) (2013), National Snow and Ice Data Center: Website. [Available at http://nsidc.org/cryosphere/sotc/sea_ice.html, Access date: September 2013.]
Nummelin, A., C. Li, and L. H. Smedsrud (2015), Response of Arctic Ocean stratification to changing runoff in a column model, *J. Geophys. Res. Oceans*, *120*, 2655–2675, doi:10.1002/2014JC010571.
Outridge, P. M., R. W. Macdonald, F. Wang, G. A. Stern, and A. P. Dastoor (2008), A mass balance inventory of mercury in the Arctic Ocean, *Environ. Chem.*, *5*(2), 89–111.
Padman, L., and T. M. Dillon (1991), Turbulent mixing near the Yermak Plateau during the coordinated Eastern Arctic Experiment, *J. Geophys. Res.*, *96*(C3), 4769–4782, doi:10.1029/90JC02260.
Panteleev, G. G., D. A. Nechaev, and M. Ikeda (2006), Reconstruction of summer Barents Sea circulation from climatological data, *Atmos. Ocean*, *44*(2), 111–132.
Pickard, G. L., and W. J. Emery (1990), Descriptive physical oceanography, Pergamon Press, Oxford, 5th ed.
Pirtle-Levy, R., J. M. Grebmeier, L. W. Cooper, and I. L. Larsen (2009), Chlorophyll *a* in Arctic sediments implies long persistence of algal pigments, *Deep Sea Res., Part II*, *56*(17), 1326–1338.
Polyak, L., et al. (2009), Late Quaternary stratigraphy and sedimentation patterns in the western Arctic Ocean, *Global Planet. Change*, *68*(1–2), 5–17.
Porter, D. F., J. J. Cassano, and M. C. Serreze (2011), Analysis of the Arctic atmospheric energy budget in WRF: A comparison with reanalyses and satellite observations, *J. Geophys. Res.*, *116*, D22108, doi:10.1029/2011JD016622.
Poulain, A. J., E. Garcia, M. Amyot, P. G. C. Campbell, and P. A. Arlya (2007), Mercury distribution, partitioning and speciation in coastal vs. inland High Arctic snow, *Geochim. Cosmochim. Acta*, *71*(14), 3419–3431.
Pucko, M., A. Burt, W. Walkusz, F. Wang, R. W. Macdonald, S. Rysgaard, D. G. Barber, J. E. Tremblay, and G. A. Stern (2014), Transformation of mercury at the bottom of the Arctic food web: An overlooked puzzle in the mercury exposure narrative, *Environ. Sci. Technol.*, *48*(13), 7280–7288, doi:10.1021/es404851b.
Rachold, V., H. Eicken, V. V. Gordeev, H. Grigoriev, H.-W. Hubberten, A. P. Lisitzin, L. Shevchenko, and L. Schirmeister (2004), Modern terrigeneous organic carbon input to the Arctic Ocean, in *The Organic Carbon Cycle in the Arctic Ocean*, edited by R. Stein and R. W. Macdonald, pp. 33–55, Springer, Berlin.
Redfield, A. C., B. H. Ketchum, and F. A. Richards (1963), The influence of organisms on the composition of seawater, in *The Sea, vol. 2*, edited by M. N. Hill, pp. 26–77, Interscience, New York.
Rice, C. P., and S. M. Chernyak (1997), Marine arctic fog: An accumulator of currently used pesticide, *Chemosphere*, *35*(4), 867–878.
Riget, F., M. P. Tamstorf, M. M. Larsen, J. Sondergaard, G. Asmund, J. M. Falk, and C. Sigsgaard (2011a), Mercury (Hg) transport in a high Arctic river in Northeast Greenland, *Water Air Soil Pollut.*, *222*(1–4), 233–242.
Riget, F., et al. (2011b), Temporal trends of Hg in Arctic biota, an update, *Sci. Total Environ.*, *409*(18), 3520–3526.
Rydberg, J., J. Klaminder, P. Rosen, and R. Bindler (2010), Climate driven release of carbon and mercury from permafrost mires increases mercury loading to sub-arctic lakes, *Sci. Total Environ.*, *408*(20), 4778–4783, doi:10.1016/j.scitotenv.2010.06.056.
Schartup, A. T., U. C. Ndu, P. H. Balcom, R. P. Mason, and E. M. Sunderland (2015a), Contrasting effects of marine and terrestrially derived dissolved organic matter on mercury speciation and bioavailability in seawater, *Environ. Sci. Technol.*, *49*(10), 5965–5972, doi:10.1021/es506274x.
Schartup, A. T., P. H. Balcom, A. L. Soerensen, K. J. Gosnell, R. S. D. Calder, R. P. Mason, and E. M. Sunderland (2015b), Freshwater discharges drive high levels of methylmercury in Arctic marine biota, *Proc. Natl. Acad. Sci. U.S.A.*, *112*(38), 11,789–11,794, doi:10.1073/pnas.1505541112.
Schroeder, W. H., K. G. Anlauf, L. A. Barrie, J. Y. Lu, A. Steffen, D. R. Schneeberger, and T. Berg (1998), Arctic springtime depletion of mercury, *Nature*, *394*(6691), 331–332.
Serreze, M. C., and R. G. Barry (2005), *The Arctic Climate System*, Cambridge Univ. Press, U. K.
Serreze, M. C., A. P. Barrett, A. G. Slater, R. A. Woodgate, K. Aagaard, R. B. Lammers, M. Steele, R. Moritz, M. Meredith, and C. M. Lee (2006), The large-scale freshwater cycle of the Arctic, *J. Geophys. Res.*, *111*, C11010, doi:10.1029/2005JC003424.
Shaw, W. J., and T. P. Stanton (2014), Vertical diffusivity of the Western Arctic Ocean halocline, *J. Geophys. Res. Oceans*, *119*, 5017–5038, doi:10.1002/2013JC009598.
Smedsrud, L. H., R. Ingvaldsen, J. E. O. Nilsen, and O. Skagseth (2010), Heat in the Barents Sea: Transport, storage, and surface fluxes, *Ocean Sci.*, *6*(1), 219–234.

Soerensen, A. L., E. M. Sunderland, C. D. Holmes, D. J. Jacob, R. M. Yantosca, H. Skov, J. H. Christensen, S. A. Strode, and R. P. Mason (2010), An improved global model for air-sea exchange of mercury: High concentrations over the North Atlantic, *Environ. Sci. Technol.*, *44*(22), 8574–8580, doi:10.1021/Es102032g.

Sommar, J., M. E. Andersson, and H. W. Jacobi (2010), Circumpolar measurements of speciated mercury, ozone and carbon monoxide in the boundary layer of the Arctic Ocean, *Atmos. Chem. Phys.*, *10*(11), 5031–5045.

Sonke, J. E., and L. E. Heimbürger (2012), Environmental science: Mercury in flux, *Nat. Geosci.*, *5*, 447–448, doi:10.1038/ngeo1508.

St Louis, V. L., M. J. Sharp, A. Steffen, A. May, J. Barker, J. L. Kirk, D. J. A. Kelly, S. E. Arnott, B. Keatley, and J. P. Smol (2005), Some sources and sinks of monomethyl and inorganic mercury on Ellesmere island in the Canadian high arctic, *Environ. Sci. Technol.*, *39*(8), 2686–2701.

St Louis, V. L., H. Hintelmann, J. A. Graydon, J. L. Kirk, J. Barker, B. Dimock, M. J. Sharp, and I. Lehnherr (2007), Methylated mercury species in Canadian high arctic marine surface waters and snowpacks, *Environ. Sci. Technol.*, *41*(18), 6433–6441.

St Pierre, K., V. L. St. Louis, J. Kirk, I. Lehnherr, S. Wang, and C. La Farge (2015), The importance of open marine waters to the enrichment of total mercury and monomethylmercury in lichens in the Canadian High Arctic, *Environ. Sci. Technol.*, *49*(10), 5930–5938, doi:10.1021/acs.est.5b00347.

Steffen, A., I. Lehnherr, A. Cole, P. Ariya, A. Dastoor, D. Durnford, J. Kirk, and M. Pilote (2015), Atmospheric mercury in the Canadian Arctic. Part I: A review of recent field measurements, *Sci. Total Environ.*, *509*, 3–15.

Stern, G. A., et al. (2012), How does climate change influence arctic mercury?, *Sci. Total Environ.*, *414*, 22–42.

Sunderland, E. M., F. A. P. C. Gobas, B. A. Branfireun, and A. Heyes (2006), Environmental controls on the speciation and distribution of mercury in coastal sediments, *Mar. Chem.*, *102*(1–2), 111–123, doi:10.1016/J.Marchem.2005.09.019.

Sunderland, E. M., D. P. Krabbenhoft, J. W. Moreau, S. A. Strode, and W. M. Landing (2009), Mercury sources, distribution, and bioavailability in the North Pacific Ocean: Insights from data and models, *Global Biogeochem. Cycles*, *23*, GB2010, doi:10.1029/2008GB003425.

Sunderland, E. M., J. Dalziel, A. Heyes, B. A. Branfireun, D. P. Krabbenhoft, and F. A. P. C. Gobas (2010), Response of a macrotidal estuary to changes in anthropogenic mercury loading between 1850 and 2000, *Environ. Sci. Technol.*, *44*(5), 1698–1704, doi:10.1021/Es9032524.

Tanhua, T., E. P. Jones, E. Jeansson, S. Jutterström, W. M. Smethie, D. W. Wallace, and L. G. Anderson (2009), Ventilation of the Arctic Ocean: Mean ages and inventories of anthropogenic CO2 and CFC-11, *J. Geophys. Res.*, *114*, C01002, doi:10.1029/2008JC004868

Toole, J. M., M. L. Timmermans, D. K. Perovich, R. A. Krishfield, A. Proshutinsky, and J. A. Richter-Menge (2010), Influences of the ocean surface mixed layer and thermohaline stratification on Arctic Sea ice in the central Canada Basin, *J. Geophys. Res.*, *115*, C10018, doi:10.1029/2009JC005660.

Trefry, J. H., R. D. Rember, R. P. Trocine, and J. S. Brown (2003), Trace metals in sediments near offshore oil exploration and production sites in the Alaskan Arctic, *Environ. Geol.*, *45*(2), 149–160.

Trefry, J. H., R. P. Trocine, L. W. Cooper, and K. H. Dunton (2014), Trace metlas and organic carbon in sediments of the northeastern Chukchi Sea, *Deep Sea Res., Part II*, in press, doi:10.1016/j.dsr2.2013.07.018.

Ullrich, S. M., T. W. Tanton, and S. A. Abdrashitova (2001), Mercury in the aquatic environment: A review of factors affecting methylation, *Crit. Rev. Environ. Sci. Technol.*, *31*(3), 241–293.

Wallace, D. W., R. M. Moore, and E. P. Jones (1987), Ventilation of the Arctic Ocean cold halocline: Rates of diapycnal and isopycnal transport, oxygen utilization and primary production inferred using chlorofluoromethane distributions, *Deep Sea Res. Part A*, *34*(12), 1957–1979.

Wang, F. Y., R. W. Macdonald, D. A. Armstrong, and G. A. Stern (2012), Total and methylated mercury in the Beaufort Sea: The role of local and recent organic remineralization, *Environ. Sci. Technol.*, *46*(21), 11,821–11,828.

Weiss-Penzias, P. S., C. Ortiz, R. P. Acosta, W. Heim, J. P. Ryan, D. Fernandez, J. L. Collett, and A. R. Flegal (2012), Total and monomethyl mercury in fog water from the central California coast, *Geophys. Res. Lett.*, *39*, L03804, doi:10.1029/2011GL050324.

Zdanowicz, C., E. M. Krummel, D. Lean, A. J. Poulain, E. Yumvihoze, J. B. Chen, and H. Hintelmann (2013), Accumulation, storage and release of atmospheric mercury in a glaciated Arctic catchment, Baffin Island, Canada, *Geochim. Cosmochim. Acta*, *107*, 316–335.

Zhang, L., L. P. Wright, and P. Blanchard (2009), A review of current knowledge concerning dry deposition of atmospheric mercury, *Atmos. Environ.*, *43*(37), 5853–5864.

Zhang, Y., D. J. Jacob, S. Dutkiewicz, H. M. Amos, and C. J. Sunderland (2015), Biogeochemical drivers of the fate of riverine mercury discharged to the global and Arctic oceans, *Global Biogeochem. Cycles*, *29*, 854–864, doi:10.1002/2015GB005124.